# Analytical and Experimental Investigations of Prestressed Laminated Composite Beams with Constrained Viscoelastic Damping Layer

V.S. Rao, B.V. Sankar, C.T. Sun, R.F. Gibson and P.R. Mantena

*Journal of Reinforced Plastics and Composites* 1994; 13; 1023
DOI: 10.1177/073168449401301104

# Analytical and Experimental Investigations of Prestressed Laminated Composite Beams with Constrained Viscoelastic Damping Layer

V. S. RAO,* B. V. SANKAR AND C. T. SUN
*Center for Studies of Advanced Structural Composites*
*Aerospace Building, P.O. Box 116250*
*University of Florida*
*Gainesville, FL 32611-6250*

R. F. GIBSON AND P. R. MANTENA**
*Department of Mechanical Engineering*
*Wayne State University*
*Detroit, MI 48202*

**ABSTRACT:** The damping characteristics of prestressed composite beams with constrained viscoelastic damping layers on one surface of the beam are investigated both analytically and experimentally. The analytical method involves derivation of finite element equations for the analysis of beam and plate structural elements with continuous or discontinuous constrained viscoelastic damping layer with prestress. The experimental method is an impulse-frequency response technique which is used on preloaded laminated beams. Results for loss factors and natural frequencies of [90/90/0/90/90] and $[90_3/0_3/90_3]$, T300/934 graphite-epoxy laminated beams with a 3M SJ-2052X constrained viscoelastic tape attached on one surface are presented. Numerical results based on the finite element prediction agree reasonably well with the experimental results under different tensile and compressive preloads.

## INTRODUCTION

LAMINATED COMPOSITE STRUCTURES used in aerospace, land and marine transportation systems often encounter dynamic load environments. Thus, it is always desirable for the composite structures to have high damping capacity. Damping physically means energy dissipation as the structure is subjected to vibratory deformations. There are a number of methods for designers to improve

*Presently with Shell Development Co., Houston, Texas.
**Presently with Mechanical Engineering Department, University of Mississippi.



0731-6844/94/11 1023-20 $6.00/0

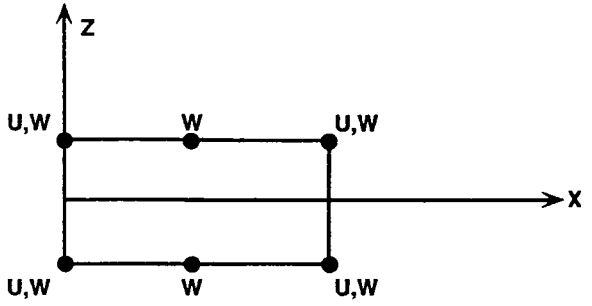


*Figure 1. Laminated offset beam element.*

damping (i.e., to take energy away from the structure). A detailed review of different damping mechanisms and the conditions under which they are effective can be found elsewhere, e.g., Nashif et al. (1985). In this paper, a method for improving damping capacity of laminated composite beams under preload using constrained viscoelastic materials externally on the beam surface is described. It appears that previous research on constrained layer damping has not included the effect of preloads.

For most viscoelastic materials, dilatation is elastic and distortion (shear) is viscoelastic (Plunket, 1983). Therefore, for viscoelastic materials, energy dissipation is primarily due to shear deformation. The main reason that constrained viscoelastic layers are used instead of unconstrained (or free) viscoelastic layers is to increase the shear deformation in the viscoelastic layer in order to improve damping. In the present research, the potential for using constrained viscoelastic materials to improve structural damping ability of laminated composite beams under prestress is examined. As shown in Figure 1, finite elements with nodes offset to either top or bottom surface of the beam are used for modeling the constrained layer and the base structure. Two-dimensional solid elements are used for modeling the viscoelastic layer sandwiched between the base structure and the constraining layer. The finite element model takes into account the preloads that are applied to the structure. An experimental technique for measuring frequencies and structural damping with prestress on the base structure is also presented. Numerical results for graphite-epoxy laminated composite beams under preload are obtained using both the analytical and experimental methods. While the experimental results were obtained at preloads beyond those required for first ply failure in the laminate, the present analytical model does not include the effects of ply failure. Nevertheless, reasonably good agreement is observed between the analysis and the experiments.

## FINITE ELEMENT FORMULATION OF STRUCTURES WITH INITIAL STRESSES

In this section, the finite element equations of a structure about a linearly prestressed configuration are developed. The formulation is based on the principle

of incremental virtual work (Fung, 1965; Bathe, 1982). Forces due to motion of the body are accounted for in the D'Alembert sense. This principle can be expressed in the following equation:

$$\int_V (T_{ij}\delta e_{ij} + \varrho \ddot{u}_i \delta u_i) dV = \int_V f_i \delta u_i dV + \int_S t_i \delta u_i dA \tag{1}$$

where

$T_{ij}$ = Cauchy stress tensor
$e_{ij}$ = infinitesimal strain tensor
$f_i$ = body force
$t_i$ = surface traction
$u_i$ = infinitesimal displacement from equilibrium configuration
$\ddot{u}_i$ = acceleration
$\varrho$ = mass density

The Cauchy stress tensor $T_{ij}$ is defined in the unknown deformed configuration. In the current configuration, in general, $T_{ij}$ cannot be obtained by simply summing the incremental stress components due to increments in strains, since rigid body rotation will change the components of Cauchy stress tensor. Therefore, for structures with preload, the second Piola-Kirchhoff stress tensor—a symmetric second order stress tensor which is essentially rotation-invariant for the small strain, large deformation case—can be used with appropriate constitutive relations.

The basic principles involved in the derivation can be found in Fung (1965) and Bathe (1982), and their application to the present problem in Rao (1991). The final form of the virtual work equation is:

$$\int_{V_0} C_{ijkl} e_{kl} \delta e_{kl} dV + \int_{V_0} {}_1S_{ij} \delta \left( \frac{1}{2} u_{k,i} u_{k,j} \right) dV + \int_{V_0} {}_0\varrho \ddot{u}_i \delta u_i dV$$

$$= \int_{V_0} f_i \delta u_i dV + \int_{\partial V_0} t_i \delta u_i dS \tag{2}$$

where $C_{ijkl}$ are the elastic coefficients and $S_{ij}$ are components of the second Piola-Kirchhoff stress tensor.

From the first term in Equation (2), the structural elastic stiffness matrix $[K_e]$ can be derived. The second term presents a stiffness matrix $[K_G]$ due to the initial loading. It should be emphasized that the $[K_G]$ matrix depends only on the preload and geometrical configuration and is independent of the material property of the element. The third term of Equation (2) is used to derive the mass matrix. The fourth term due to the effect of the body force can be omitted and the fifth

term is due to the surface loading on the beam. In the following section, derivations of element matrices of constrained beams with prestress will be presented.

## DERIVATIONS FOR CONSTRAINED COMPOSITE BEAMS

The base structure and the constraining layer are modeled with offset beam elements (Sankar, 1991) and the viscoelastic core is modeled with two-dimensional plane solid elements.

### Laminated Offset Beam Element

The element can be described as a three-node, seven-degree-of-freedom offset beam element as shown in Figure 1. In Figure 1, $u$ is the nodal displacements in the $x$-direction, $w$ is the nodal displacements in the $z$-direction and $\psi$ is the rotation about the $y$-axis of a line normal to the $x$-axis. The element is shear-deformable, which is important in modeling fiber-reinforced composites. The offset ability allows for the beam nodes to be offset to one surface of the beam, so that they coincide with the nodes of the adjoining element on the surface of the beam. The assumed displacement field is

$$\begin{aligned} u(x,z) &= u_0(x) - z\psi(x) \\ w(x,z) &= w(x) \\ \psi(x,z) &= \psi(x) \end{aligned} \tag{3}$$

In Equation (3) $u_0$ and $\psi$ are defined by using linear interpolation functions

$$\begin{aligned} u(x) &= \begin{bmatrix} \frac{1-x}{2} & 0 & \frac{1+x}{2} \end{bmatrix} [u_1^e \quad 0 \quad u_3^e]^T \\ \psi(x) &= \begin{bmatrix} \frac{1-x}{2} & 0 & \frac{1+x}{2} \end{bmatrix} [\psi_1^e \quad 0 \quad \psi_3^e]^T \end{aligned} \tag{4}$$

where $u_1$, $u_3$, $\psi_1$ and $\psi_3$ are corresponding nodal displacements. The transverse deformation $w$ is defined by using quadratic interpolation functions

$$w(x) = \begin{bmatrix} x(x-1)/2 \\ 1 - x^2 \\ x(x+1)/2 \end{bmatrix}^T \begin{Bmatrix} w_1^e \\ w_2^e \\ w_3^e \end{Bmatrix} \tag{5}$$

where $w_i^e$ $(i = 1,2,3)$ are nodal displacements. The non-zero strain components are obtained from the strain-displacement relations

$$\begin{Bmatrix} e_{xx} \\ e_{xz} \end{Bmatrix} = \begin{Bmatrix} u_{0,x} \\ w_{,x} + \psi \end{Bmatrix} - z \begin{Bmatrix} \psi_{,x} \\ 0 \end{Bmatrix} \tag{6}$$

The non-zero stress components are expressed in displacement components in the form

$$\begin{Bmatrix} \sigma_{xx} \\ \sigma_{xz} \end{Bmatrix} = \begin{bmatrix} Q & 0 \\ 0 & Q_s \end{bmatrix} \left[ \begin{Bmatrix} u_{0,x} \\ W_{,x} - \psi \end{Bmatrix} - z \begin{Bmatrix} \psi_{,x} \\ 0 \end{Bmatrix} \right] \tag{7}$$

*ELEMENT STIFFNESS MATRIX [K]*

By using Equations (6) and (7), the first term of the virtual work expression of Equation (2) can be written in matrix form as

$$\int_{V_0} C_{ijkl} e_{ke} \delta e_{ij} dV = \int_A \{\delta E\}[G]\{E\} dA \tag{8}$$

where the vector $\{E\}$ and the matrix $[G]$ are given by

$$\{E\} = \begin{Bmatrix} u_{0,x} \\ w_{,x} - \psi \\ \psi_{,x} \end{Bmatrix}$$

$$[G] = \begin{bmatrix} A & B & 0 \\ B & D & 0 \\ 0 & 0 & F \end{bmatrix} \tag{9}$$

$$(A, B, D, F) = \int_{z_0 - h/2}^{z_0 + h/2} (Q, zQ, z^2 Q, Q_s) dz \tag{10}$$

The element stiffness matrix due to incremental strain is derived from

$$\int_{V_0} c_{ijkl} e_{kl} \delta e_{ij} dV = \int_A \{\delta E\}[G]\{E\} dA$$

$$= \int_A \{\delta U\}^{eT} [N]^T [P]^T [G][P][N]\{U\}^e dA$$

$$= \{\delta U\}^{eT} [K]\{U\}^e \tag{11}$$

A 3 × 3 Gaussian quadrature can be used to reliably evaluate the element stiffness matrix. In Equation (11), $[N]$ is an interpolation function matrix and $[P]$ is a matrix of partial differential operators. Their detailed expressions for $[N]$ and $[P]$ are given in Bathe (1982), and documented in Rao (1991).

*INITIAL STRESS MATRIX [$K_G$]*

The presence of an initial stress in a structure modifies the stiffness of the structure. Physically, this effect represents the coupling between the in-plane and out-of-plane deformations. The second term in Equation (2) can be written in matrix form

$$\int_{V_0} {}_1S_{ij}\delta\left(\frac{1}{2}u_{k,i}u_{k,j}\right)dV = \int_{V_0} \delta u_{i,j}u_{i,k}\,{}_1S_{j,k}dV$$

$$= \int_{V_0} \{\delta\bar{E}\}^T[S]\{\bar{E}\}dV \tag{12}$$

where ${}_1[S]$ is the initial stress matrix and is given by

$${}_1[S] = \begin{bmatrix} S & 0 & 0 \\ 0 & S & 0 \\ 0 & 0 & S \end{bmatrix} \tag{13}$$

$$\{\bar{E}\} = \{\bar{E}_1\} - z\{\bar{E}_2\} = \begin{Bmatrix} u_{0,x} \\ w_{,x} \\ \psi_{,x} \end{Bmatrix} - z\begin{Bmatrix} 0 \\ \psi \\ 0 \end{Bmatrix} \tag{14}$$

By substituting Equations (13) and (14) into (12) we obtain

$$\int_{V_0} \{\delta\bar{E}\}^T{}_1[S]\{\bar{E}\}dV = \int_A \{\delta\bar{E}_1\}^T[\bar{N}]\{\bar{E}_1\}dA - \int_A \{\delta\bar{E}_2\}^T[\bar{M}]\{\bar{E}_1\}dA$$

$$- \int_A \{\delta\bar{E}_1\}^T[\bar{M}]\{\bar{E}_2\}dA + \int_A \{\delta\bar{E}_2\}^T[\bar{Z}]\{\bar{E}_2\}dA \tag{15}$$

where

$$[\bar{N}] = \int_{z_0-(h/2)}^{z_0+(h/2)} {}_1[S]\,dz$$

$$[\bar{M}] = \int_{z_0-(h/2)}^{z_0+(h/2)} {}_1[S]\,z\,dz \tag{16}$$

$$[\bar{Z}] = \int_{z_0-(h/2)}^{z_0+(h/2)} {}_1[S]\,z^2\,dz$$

In terms of nodal displacements, the second term can be written as

$$\int_{V_0} S_{ij}\delta\zeta_{ij}dV = \int_{V_0} \{\delta\bar{E}\}^T[S]\{\bar{E}\}dV = \int_A \begin{Bmatrix} \delta\bar{E}_1 \\ -\delta\bar{E}_2 \end{Bmatrix}^T \begin{bmatrix} \bar{N} & \bar{M} \\ \bar{M} & \bar{Z} \end{bmatrix} \begin{Bmatrix} \bar{E}_1 \\ -\bar{E}_2 \end{Bmatrix} dA$$

$$= \int_A \{\delta U\}^{eT}[N]^T[\bar{P}]^T \begin{bmatrix} \bar{N} & \bar{M} \\ \bar{M} & \bar{Z} \end{bmatrix} [\bar{P}]^T[N]\{U\}^e dA$$

$$= \{\delta U\}^{eT}[K_G]\{U\}^e \tag{17}$$

The geometric stiffness matrix can be evaluated by using the Gaussian quadrature scheme, as in the case of the elastic stiffness matrix $[K]^e$.

*MASS MATRIX*

The mass matrix $[M]$ is calculated in a similar manner from the third term of Equation (2). The difference between the present derivation and the formulation for conventional elements is due to the offset factor. The acceleration field $\{\ddot{u}\}$ is approximated by using the same interpolation functions $[N]$ that were used for the displacement field $\{u\}$, i.e., within each element we can write

$$\{u\} = [N]\{U\}^e, \qquad \{\ddot{u}\} = [N]\{\ddot{U}\}^e \tag{18}$$

Using Equation (18), the third term of Equation (2) becomes

$$\int_{V_0} \varrho_0 \delta u_i \ddot{u}_i dV = \int_{V_0} \varrho_0 \{\delta U\}^T\{\ddot{U}\}dV \tag{19}$$

where

$$\{\delta U\} = \begin{Bmatrix} \delta u \\ \delta w \end{Bmatrix} = [A]\{\delta\bar{U}\}$$

$$= \begin{bmatrix} 1 & 0 & z \\ 0 & 1 & 0 \end{bmatrix} \begin{Bmatrix} \delta u_0 \\ \delta w \\ \delta\psi \end{Bmatrix} \tag{20}$$

$$[\ddot{U}] = \begin{Bmatrix} \ddot{u} \\ \ddot{w} \end{Bmatrix}$$

From Equations (18)–(20) we obtain

$$\int_{V_0} \varrho_0 \{\delta U\}^T\{\ddot{U}\}dV = \int_{V_0} \varrho_0 \{\delta U\}^T[N]^T[A]^T[A][N]\{\ddot{u}\}dV$$

$$= \{\delta U\}^T [M] \{\ddot{U}\} \tag{21}$$

Therefore, the consistent element mass matrix can be calculated from the expression

$$[M] = h \int_A \varrho_0 [N]^T [\bar{A}] [N] dA \tag{22}$$

The entries in $[\bar{A}]$ are given by

$$[\bar{A}] = \int_{z_0+(h/2)}^{z_0-(h/2)} [A]^T [A] dA \tag{23}$$

## Six-Node Isoparametric Plane Solid Element

The plane solid element was derived to model the viscoelastic damping layer in damped sandwich beams, so it is required to be compatible with the laminated offset beam element (see Figure 2). The plane element is a six-node ten-degree-of-freedom element and is shown in Figure 3. In order to be compatible with the beam element, the order of interpolation functions was chosen as described below. The displacements $u$ in the $x$-direction were interpolated by using linear interpolation functions of $x$ and $z$. The nodal displacements in the $z$ direction, $w$, were interpolated using quadratic interpolation functions in the $x$-direction and linear interpolation functions in the $z$-direction. The use of higher order interpolation for $w$ in the $x$-direction improves the performance of the element in situations where the loading causes $w$ to be much larger than $u$, as in beam bending problems.

### *ELASTIC STIFFNESS MATRIX AND MASS MATRIX*

A detailed development of the elastic element stiffness and the mass matrix for the plane elements in general can be found in Bathe (1985), and particularly for this element in Rao (1991). Only a brief derivation is included in this section.

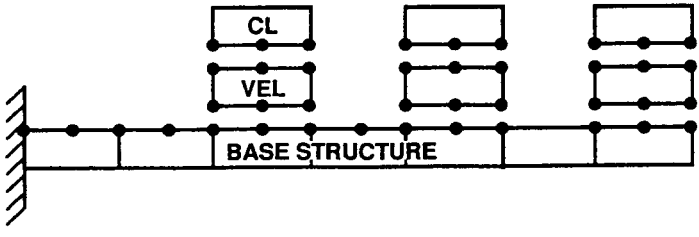


***Figure 2.*** *Damped beam finite element model.*

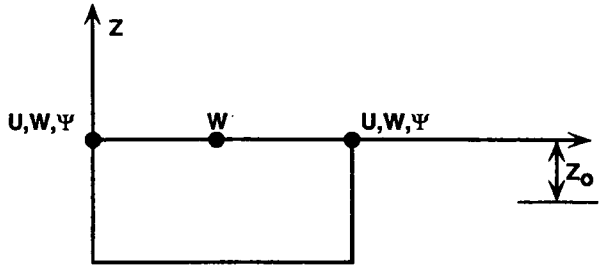


***Figure 3.*** *Two-dimensional plane solid.*

Within each element, the displacement field is assumed to be of the form

$$\{u\} = [N]\{U\}^e \tag{24}$$

where $[N]$ is the matrix of interpolation function, and $\{U\}^e$ is the vector of elemental degrees of freedom.

As in the development of the elastic stiffness matrix $[K]^e$ of the offset beam element, we can still use the general expression

$$\int_{V_0} c_{ijkl} e_{ij} \delta e_{kl} dV = \int_A \{\delta U\}^{eT} [N]^T [P]^T [G][P][N]\{U\}^e dA$$

$$= \{\delta U\}^{eT} [K]^e \{U\}^e \tag{25}$$

where $[P]$ is the matrix of differential operators and $[G]$ the constitutive matrix for an isotropic material:

$$[G] = \frac{E}{1-\nu^2} \begin{bmatrix} 1 & \nu & 0 \\ \nu & 1 & 0 \\ 0 & 0 & \dfrac{1-\nu}{2} \end{bmatrix}$$

$$[P] = \begin{bmatrix} \dfrac{\partial}{\partial x} & 0 & 0 \\ 0 & 0 & \dfrac{\partial}{\partial z} \\ \dfrac{\partial}{\partial z} & 0 & \dfrac{\partial}{\partial x} \end{bmatrix}$$

The element stiffness matrix $[K]^e$, after making appropriate substitution into Equation (25), can be derived in terms of $[N]$, $[P]$ and $[G]$:

$$[K]^e = \int_{V_0} [N]^T [P]^T [G] [P] [N] dV \tag{26}$$

The element mass matrix $[M]$, after making appropriate substitution in the third term of Equation (2), is derived as

$$[M]^e = \int_{V_0} e_0 [N]^T [N] dV \tag{27}$$

The $[K]^e$ and $[M]^e$ matrices are calculated by using an appropriate Gaussian quadrature rule.

*INITIAL STRESS MATRIX*

The initial stress stiffness matrix $[K_G]$ of the plane solid element is calculated from the second term in Equation (2):

$$\int_{V_0} {}_1S_{ij} \delta\zeta_{ij} dV = \int_{V_0} \delta u_{i,j} u_{i,k} {}_1S_{j,k} dV$$

$$= \int_{V_0} \{\bar{E}\}^T {}_1[S] \{\bar{E}\} dV$$

$$= \int_A \{\delta U\}^{eT} [N]^T [\bar{P}]^T {}_1[S] [\bar{P}] [N] \{U\}^e dA$$

$$= \{\delta U\}^{eT} [K_G] \{U\}^e \tag{28}$$

where

$$\{\bar{E}\} = \begin{Bmatrix} u_x \\ u_z \\ w_x \\ w_z \end{Bmatrix} \tag{29}$$

$${}_1[S] = \begin{bmatrix} S & 0 \\ 0 & S \end{bmatrix} \tag{30}$$

and $[\bar{P}]$ is the matrix of differential operators such that

$$\{\bar{E}\} = [\bar{P}][N]\{U\}^e \tag{31}$$

## CALCULATION OF LOSS FACTOR

The loss factor $\eta$ of a structure executing steady state vibration is defined in terms of energy as

$$\eta = \frac{D}{2\pi W} \tag{32}$$

where $D$ is the energy dissipated per cycle and $W$ is the maximum (peak) energy stored in the structure. In general there are two approaches which are commonly used to evaluate the loss factor $\eta$ from our finite element program. These approaches will be discussed in this section.

### Direct Frequency Response Method

In the direct frequency response method, a forced vibration over a range of frequencies is considered, and a theoretical response spectrum is generated from which the overall damping of the system is calculated. For the forced vibration problem, the objective is to predict the linear, damped, steady-state response of structures about a linear preloaded equilibrium configuration. Since the core material is viscoelastic, the complex modulus approach is used and the governing differential equations are complex. Following finite element discretization, the equations governing the time dependent response of a prestressed body are obtained as

$$[[K] + [K_G]]\{U\} + [M]\{\ddot{U}\} = \{F\} \tag{33}$$

where

$[K]$ = global complex stiffness matrix
$[K_g]$ = global geometric stiffness matrix
$[M]$ = global mass matrix
$\{U\}$ = global displacement vector (complex)
$\{\ddot{U}\}$ = global acceleration vector (complex)

A harmonic excitation force is considered, i.e.,

$$F = fe^{iwt} \tag{34}$$

where $\omega$ is the forcing frequency, $t$ is the time and $i = (-1)^{1/2}$. The response due to the applied force is assumed to be harmonic and at the excitation frequency. The equation of motion reduces to

$$[[K] + [K_G]]\{U\} - \omega^2[M]\{U\} = \{f\} \tag{35}$$

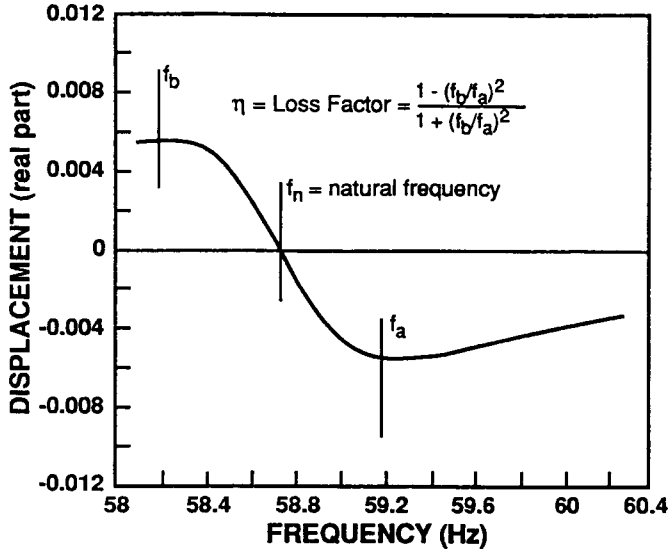


***Figure 4.*** *Real part of the response spectrum near a natural frequency.*

The matrix on the left hand side is called the displacement impedance matrix. For each frequency of excitation, the displacement per unit applied force is calculated by solving the system of complex-valued simultaneous linear equations, and the response function is thereby generated. Loss factor is calculated by using a single degree-of-freedom curve-fitting approach on the real part of the generated response spectrum as shown in Figure 4.

## Modal Strain Energy Approach

The second technique is based on an eigenvalue problem which is derived by setting the forcing terms to zero, i.e.,

$$[[K] + [K_G]]\{U\} = \omega^2[M]\{U\} \tag{36}$$

The analysis can be performed based on the associated complex eigenvalue problem or the simplified real eigenvalue problem. In the complex eigenvalue method, the resonant frequencies and complex mode shapes of the damped system are determined by solving the complex eigenvalue problem. The loss factor for vibration about a prestressed configuration is calculated by

$$\eta = \sum_{i=1}^{i=n} \eta_i E_i^m \Bigg| \sum_{i=1}^{i=n} E_i \tag{37}$$

where

$n$ = total number of elements
$\eta_i$ = loss factor of the $i$th element
$E_i^m$ = elastic strain energy stored in $i$th element calculated as $1/2\ \{u\}^T[K]\{u\}$
$E_i$ = sum of elastic strain energy and strain energy due to preload in the $i$th element calculated as $1/2\ \{u\}^T[K + K_G]\{u\}$

In general, the modal methods provide information about a basic and more general behavior of the damped structure, over a wide frequency range, without accounting for the actual loading situation. The direct frequency response method will provide detailed response information in the specified range of interest. In this paper the modal strain energy method was used to determine the loss factor $\eta$.

The variation of material properties of the viscoelastic damping material with frequency is very pronounced, and in eigenvalue-based techniques, the frequencies of interest are not known a priori. Therefore, an iterative procedure has to be used, starting with a rough estimate of resonant frequencies. The material properties of the viscoelastic material are updated corresponding to the calculated resonant frequencies. The procedure is repeated to convergence for each mode of interest. System loss factors calculated without iterating will produce correspondingly inaccurate results. This is one problem which is avoided in the direct frequency method, since the loading frequency is known ahead of time.

## EXPERIMENTAL INVESTIGATION

The objective of the experimental program was to measure the effects of axial preloads on the flexural frequencies and loss factors of composite specimens with and without surface damping treatments. Although it was decided that experiments would include preloads beyond those required for first ply failure, it was realized that the analytical model might not be valid after such failures. Two different types of specimens were designed and fabricated from unidirectional Fiberite T300/934 graphite/epoxy prepreg tape using an autoclave-style press and the manufacturers' recommended cure cycle (Gibson, Deobald and Suarez, 1985). One specimen type was designed to produce data for tensile loading beyond first ply failure, while the other specimen type was designed to produce data under both tensile and compressive preloads in the linear range below first ply failure. In both cases, the surface damping treatment was 3M SJ-2052X damping tape having a 0.005 inch (0.127 mm) thick ISD 112 acrylic polymer viscoelastic adhesive and a 0.01 inch (0.254 mm) thick dead soft aluminum backing as the constraining layer. The damping tape was applied on one side of the composite specimen along the full length of the specimen between the clamping fixtures in the testing machine.

The first type of specimen was a 5 ply $[90_2/0/90_2]$ laminate which was designed to be loaded up to and beyond first ply failure in a Monsanto Tensometer 20, a benchtop universal testing machine (Figure 5). In order to determine the effects

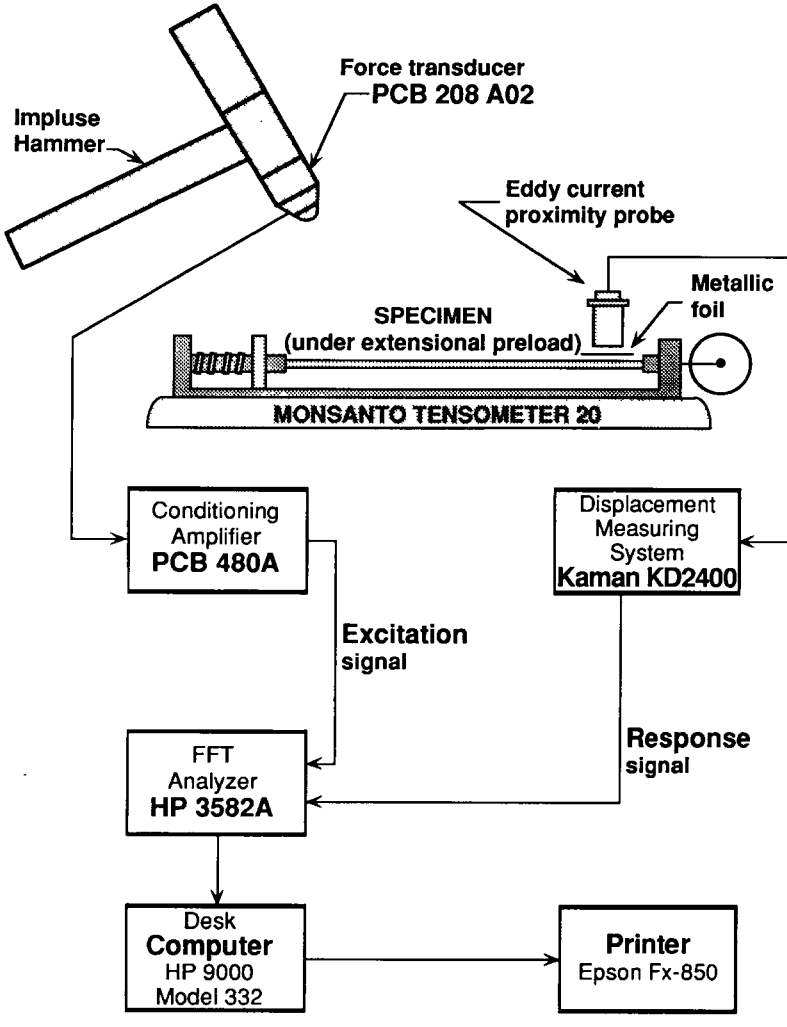


***Figure 5.*** *Apparatus for impulse-frequency response testing prestressed flexural specimens.*

of first ply failure on the frequencies and damping of the composite structure, the transverse (90°) plies were placed on the outer surfaces of the specimens for visual observation of first ply failure. Such a thin laminate would also ensure that the first ply failure loads would be low, and that resulting friction damping in the specimen clamping fixtures would be minimized.

A second type of specimen was used to generate experimental data on frequencies and damping under both tensile and compressive preloads for comparison with the finite element predictions. The first type of specimen would not be suitable for these experiments because the buckling load under compressive preload is too low. A thicker laminate was required in order to withstand both tensile and compressive preloads. Thus, it was decided that the second type of specimen would be an 18 ply $[90_3/0_3/90_3]_s$ laminate.

In both types of specimens, load transfer shoulders consisting of Epon 828 epoxy resin/V40 hardener (100:80 parts by weight) were molded on the ends of the specimens to match machined notches in the clamping fixtures. The shoulders were designed to have shear strengths greater than the predicted composite first ply failure loads.

Frequencies and loss factors were measured using an impulse-frequency response technique which has been described in detail in previous publications, e.g., Suarez and Gibson (1987). The same technique has also been used to study the effects of surface damping treatments on composite structures without preloads (Mantena, Gibson and Hwang, 1989). Material property data for specimens and damping tape are also given in the above reference. In the current application, the preloaded specimen is excited in flexural vibration using an impulse hammer which has a piezoelectric force transducer in its tip (Figure 5). The specimen response is measured by a non-contacting eddy current proximity transducer, and both signals are fed into a frequency spectrum analyzer. By using the half-power bandwidth method at the resonant peaks in the frequency response function, the resonant frequency and the loss factor are determined.

## RESULTS AND DISCUSSION

Structural damping of composite beams subjected to an axial preload was evaluated by using the finite-element approach described in the previous sections and the modal strain energy method. Some of the results were compared with the experimental results. Results of effects of different parameters such as length of the damping treatment and preload, on the overall damping of the composite beam were presented.

Figures 6 and 7 show the effect of preload on frequency and loss factor (damping) for a 3M's SJ-2052X damping tape starting at the fixed end ($a = 0$) with a length of $0.4L$ ($b = 0.4L$, $L$ = length of the beam) of the graphite-epoxy composite beam of stacking sequence [90/90/0/90/90], length 0.2032 m, width 0.01905 m and thickness of 0.00064 m. For the static part of the loading, the beam is fixed at one end with an axial load acting at the free end, and for the dynamic part of the loading, the beam is fixed at both ends in Figure 6 and fixed-hinged ends in Figure 7. From Figures 6 and 7 we notice that damping decreases with

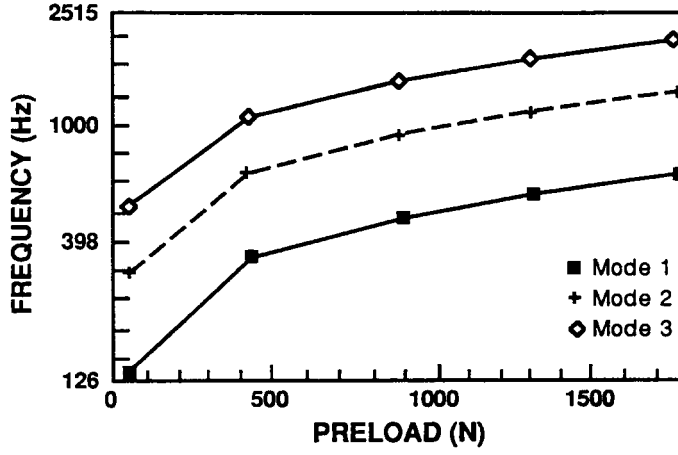


***Figure 6.*** *Variation of frequency with preload.*

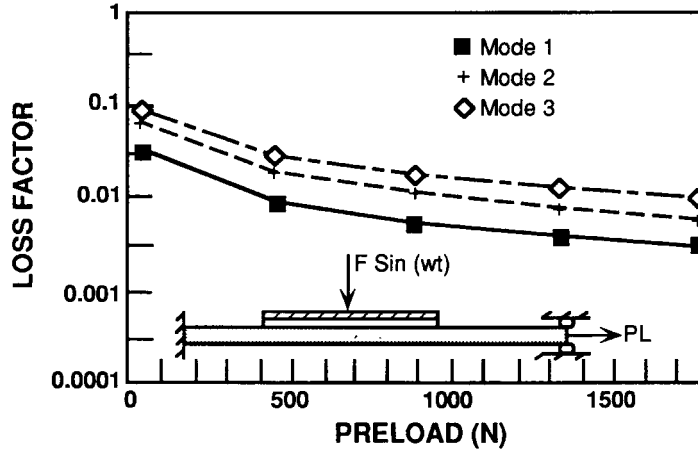


***Figure 7.*** *Variation of loss factor with preload.*

increasing preload and the frequency (or stiffness) increases at the same time. Decreased loss factor alone does not necessarily result in increased vibration amplitude since dynamic response depends on both stiffness and damping. However, for a given preload, the displacement is always considerably smaller when damping treatment is present. More numerical results for different values of $a$ and $b$, which show the effects of preload on loss factor and frequency can be found in Rao (1991).

Figure 8 shows the experimentally determined effects of tensile preload on flexural damping and first mode flexural frequency, respectively, for the 5 ply $[90_2/0/90_2]$ graphite/epoxy specimens. For the untaped specimen, the loss factor shows an initial drop of about 70% under axial loading up to about 65% of the estimated first ply failure load. The loss factor then steadily increases until the load is beyond the estimated first ply failure load. This increase is thought to be due to matrix crack damage in the outer transverse plies, which we have observed in previous research as well (Mantena, Place and Gibson, 1985). Cracking sounds were also noticed at around 80% of the estimated first ply failure load. With the damping tape applied, the change in loss factor with load in Figure 8 is initially the same as without tape. The loss factor does not increase after first ply failure, however. This is probably due to the fact that the baseline damping due to the tape is high enough to mask out any increases due to matrix cracking in the composite base structure. This is further proof of the importance of the damping treatment.

As shown in Figure 8, the increases in resonant frequency with increasing axial preload were quite large, with upward shifts of about 250% at the estimated first ply failure load. Changes in frequency of such a flexible member under axial load can be predicted quite accurately by using a one-dimensional wave equation for a vibrating string under tension—the natural frequency turns out to be proportional to the square root of the tensile load.

In order to help explain the experimental results on the effects of preload, the effects of both tensile and compressive axial preloads on damping and frequency of $[90_3/0_3/90_3]$, graphite epoxy specimens with and without SJ-2052X damping tape were determined both experimentally and analytically. Analytical results from the University of Florida finite element model and modal strain energy method are compared with experimental results from Wayne State University in Figure 9. Experimental and analytical results show, with good agreement, that with increasing tensile preload, the loss factor decreases and the frequency increases. An increasing compressive preload has the opposite effect. Similar results were reported for viscoelastic sandwich beams by Sato et al. (1986). There is consistently more scatter in the experimental data for compressive loading, possibly because of inherent instability of the compressively loaded system. The crossover of curves for frequency versus compressive preload with and without tape is seen in both analytical and experimental results. The agreement between experimental results and theoretical predictions is very encouraging.

Finally the finite element program can also be expanded to laminated plates with constrained viscoelastic damping layers. Further development of the finite element program and the numerical results will be presented in the near future.

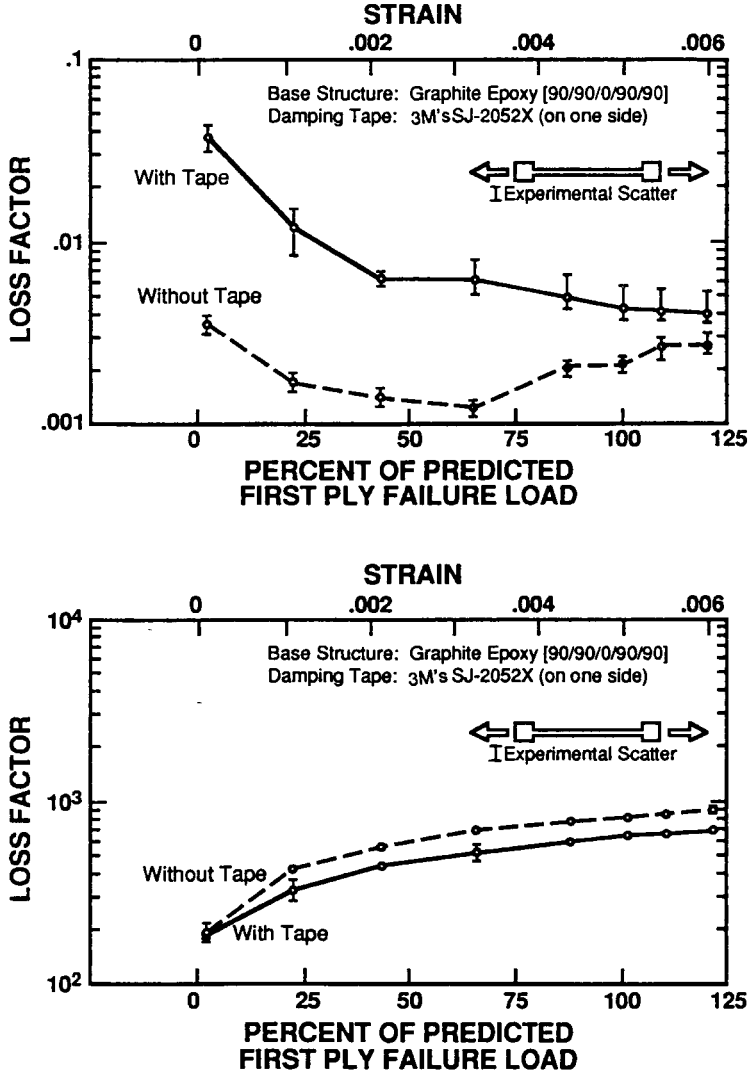


***Figure 8.*** *Effect of axial preloads on natural frequency and loss factor of graphite/epoxy specimens with and without damping tapes.*

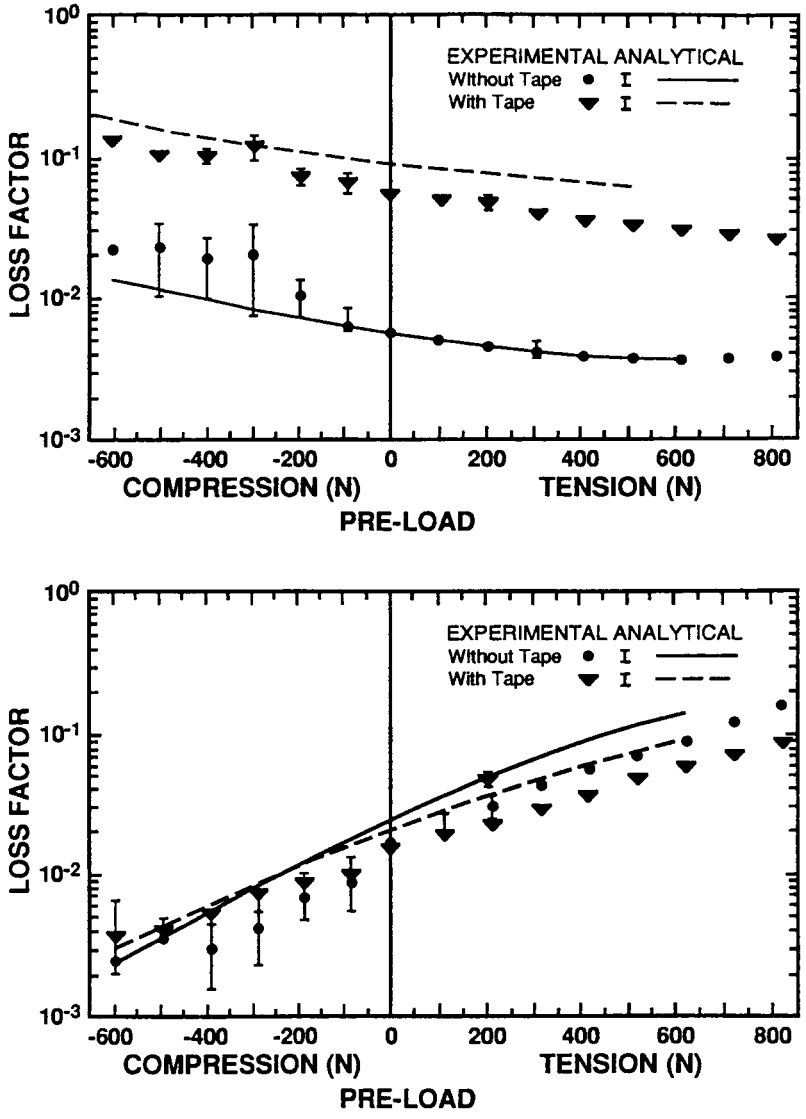


***Figure 9.*** *Comparison of experimental and finite element analysis results on effects of tensile and compressive axial preloads.*

## ACKNOWLEDGEMENTS

This research was sponsored by the Army Research Office under Contract No. DAAL03-88-K0013 monitored by Dr. Gary L. Anderson. The assistance of A. Murthy Lakshminarayan, graduate assistant at Wayne State University, is also gratefully acknowledged.

## REFERENCES

Bathe, K. J. 1982. *Finite Element Procedures in Engineering Analysis.* Englewood Cliffs, NJ: Prentice-Hall, Inc.

Fung, Y. C. 1965. *Foundation of Solid Mechanics.* Englewood Cliffs, NJ: Prentice-Hall, Inc.

Gibson, R. F., L. R. Deobald and S. A. Suarez. 1985. "Laboratory Production of Discontinuous Aligned Composite Plates Using the Autoclave-Style Press Cure," *Journal of Composites Technology and Research,* 7(2):49–54.

Mantena, P. R., R. F. Gibson and S. J. Hwang. 1989. "Optimal Constrained Viscoelastic Tape Lengths for Maximizing Damping in Laminated Composites," presented at *Damping 89 Symposium,* West Palm Beach, FL, Feb. 8–10.

Mantena, P. R., T. A. Place and R. F. Gibson. 1985. "Characterization of Matrix Cracking in Composite Laminates by the Use of Damping Capacity Measurements," in *Role of Interfaces on Material Damping.* Park, OH: ASM International, pp. 79–94.

Nashif, A. D., D. I. G. Jones and J. P. Henderson. 1985. *Vibration Damping.* New York: John Wiley.

Plunkett, R. 1983. "Damping Mechanism in Fiber Reinforced Laminates," *Proceedings of IVTAM Conference on Advances in Composite Materials.* Oxford: Pergamon, pp. 93–104.

Rao, V. S. 1991. "Finite Element Analysis of Viscoelastically Damped Composite Structures," Ph.D. dissertation, Department of Aerospace Engineering, Mechanics and Engineering Science, University of Florida, Gainesville.

Sankar, B. V. 1991. "A Finite Element for Modeling Delaminations in Composite Beams," *Computers and Structures,* 38(2):239–246.

Sato, K., G. Shikanai and T. Tainaka. 1986. "Damping of Flexural Vibration of Viscoelastic Sandwich Beam Subjected to Axial Force," *Bulletin of Japanese Society of Mechanical Engineers,* 29(253): 2204–2210.

Suarez, S. A. and R. F. Gibson. 1987. "Improved Impulse-Frequency Response Techniques for Measurement of Dynamic Mechanical Properties of Composite Materials," *Journal of Testing and Evaluation,* 15(2):114–121.

Suarez, S. A., R. F. Gibson and L. R. Deobald. 1983. "Development of Experimental Techniques for Measurement of Damping in Composite Materials," *Proceedings of the Society of Experimental Stress Analysis Meeting,* Salt Lake City, UT, Nov. 6–10, pp. 55–60.